Behavioral/Systems/Cognitive

# A Cholinergic Gating Mechanism Controlled by Competitive Interactions in the Optic Tectum of the Pigeon

**Gonzalo Marín,[1] Carlos Salas,[1] Elisa Sentis,[1] Ximena Rojas,[2] Juan Carlos Letelier,[1] and Jorge Mpodozis[1]**

[1]Departamento de Biología, Facultad de Ciencias and [2]Programa de Morfología, Facultad de Medicina, Universidad de Chile, Santiago, Chile

**We describe the operation of a midbrain neural circuit in pigeons that may participate in selecting and attending to one visual stimulus from the myriad displayed in their visual environment. This mechanism is based on a topographically organized cholinergic signal reentering the optic tectum (TeO). We have shown previously that, whenever a visual stimulus activates neurons in a given tectal location, this location receives a strong bursting feedback from cholinergic neurons of the nucleus isthmi pars parvocellularis (Ipc), situated underneath the tectum. Here we show that, if a second visual stimulus is presented, even far from the first, the feedback signal to the first tectal location is diminished or suppressed, and feedback to the second tectal location is initiated. We found that this long-range suppressive interaction is mostly mediated by the nucleus isthmi pars magnocellularis, which sends a wide-field GABAergic projection to Ipc and TeO. In addition, two sets of findings indicate that the feedback from the Ipc modulates the ascending output from the TeO. First, visually evoked extracellular responses recorded in the dorsal anterior subdivision of the thalamic nucleus rotundus (RtDa), receiving the ascending tectal output, are closely synchronized to this feedback signal. Second, local inactivation of the Ipc prevents visual responses in RtDa to visual targets moving in the corresponding region of visual space. These results suggest that the ascending transmission of visual activity through the tectofugal pathway is gated by this cholinergic re-entrant signal, whose location within the tectal visual map is dynamically defined by competitive interactions.**

*Key words:* **spatial attention; cholinergic; winner-take-all; optic tectum; superior colliculus; isthmi**

## Introduction

Spatial attention enhances visual processing at circumscribed locations of visual space (Posner, 1980). Accordingly, in several visual areas attending to one location enhances neuronal responses to stimuli presented at that location and suppresses responses to unattended regions (Desimone and Duncan, 1995; Maunsell and Cook, 2002). This gating effect of spatial attention likely depends on local facilitation mechanisms and wide-field competitive interactions, presumably acting at many different neural levels (Deco et al., 2002). The superior colliculus (SC) is one structure in which these processes may take place, because it seems crucially involved in the selection of salient visual stimuli becoming the focus of attention and the target of subsequent orienting responses (Carello and Krauzlis, 2004; Cavanaugh and Wurtz, 2004; Muller et al., 2005).

From experiments in the pigeon optic tectum (TeO) (homologous to the SC), we have proposed that a focal gating of incoming visual stimuli may result from a topographically organized cholinergic feedback, whose location within the tectal visual map is defined by competitive interactions (Marin et al., 2005). This focal mechanism would be mediated by the nuclei isthmi pars parvocellularis (Ipc) and pars magnocellularis (Imc), both reciprocally connected to TeO (Wang et al., 2006). The cholinergic feedback is manifested by visually evoked oscillatory bursting potentials (OBs) recorded across tectal layers, generated by the bursting firing of "paintbrush" axon terminals from Ipc neurons (Marín et al., 2005). Activity in separate locations may compete via long-range GABAergic connections made by Imc neurons on most of the Ipc and the tectum (see Fig. 1) (Wang et al., 2004).

Although columnar paintbrush terminals may release acetylcholine across several tectal layers, their main effect could likely be on type I tectal ganglion cells (TGCs) (Wang et al., 2006). These neurons possess large dendritic arborizations that terminate in dendritic specializations (bottlebrushes) arranged in a single tectal layer, specific for different types of TGCs (Luksch et al., 1998). Ipc paintbrush terminals are particularly dense in tectal layer 5, intermingling with both retinal axon terminals and dendritic bottlebrushes of type I TGCs (Wang et al., 2006). Type I TGCs project to central and dorsoanterior subdivisions of the thalamic nucleus rotundus (Rt) (caudal pulvinar in mammals) (Karten et al., 1997; Major et al., 2000), in a highly convergent manner (Marín et al., 2003), producing large, motion-sensitive receptive fields (RFs) in Rt neurons (Wang et al., 1993).

Here we show that visually triggered cholinergic feedback impinging on one tectal locus competes with feedback produced in other activated loci via long-distance suppressive interactions mediated by Imc. We also show that visually evoked extracellular responses of the dorsoanterior subdivision of the rotundus

Received March 29, 2007; revised May 30, 2007; accepted June 18, 2007.

This work was supported by Fondecyt Grants 1061108 (J.C.L.) and 1030522 (J.M.). We thank Josh Wallman for valuable comments and substantial help in preparing this manuscript. We also thank Diane Greenstein for editorial assistance.

Correspondence should be addressed to Gonzalo Marín, Departamento de Biología, Facultad de Ciencias, Universidad de Chile, Las Palmeras 3425, Ñuñoa, Santiago, Chile. E-mail: gmarin@uchile.cl.

DOI:10.1523/JNEUROSCI.1420-07.2007

 0270-6474/07/278112-10$15.00/0

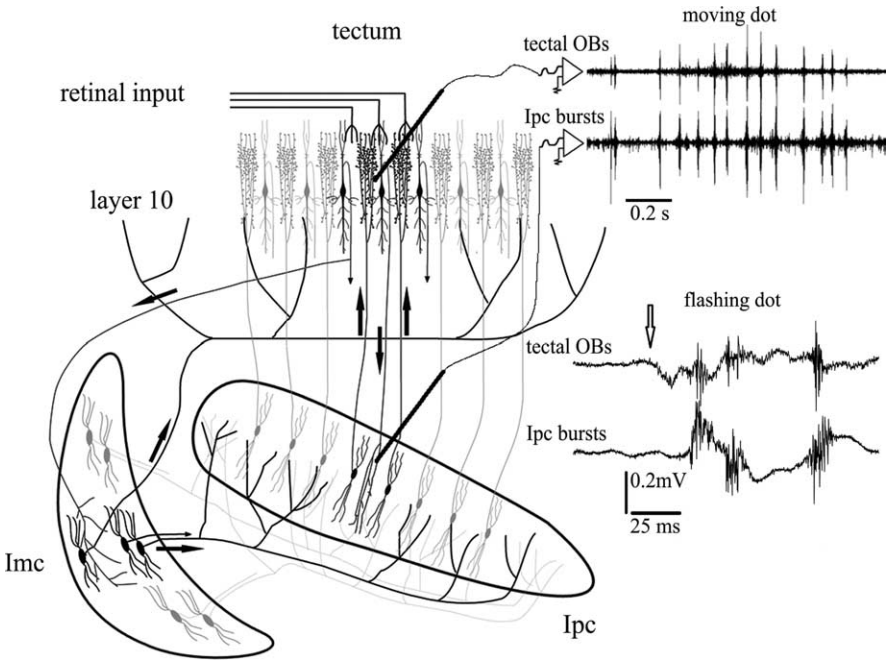


**Figure 1.** Tectal OBs represent re-entrant signals coming from Ipc. Schematic illustrating the synaptic connectivity between the isthmi and TeO. Neurons in the Ipc receive a topographically organized visual input from shepherd-crook neurons of tectal layer 10 and project back to the homotopic location via cholinergic paintbrush axon terminals. Imc neurons receive a coarser projection from shepherd-crook neurons and send widely ramifying, GABAergic terminal fields on most of the Ipc and TeO. Recording traces show mirror-like pattern of bursting responses recorded at homotopic locations in the Ipc and TeO. Moving (40°/s) or flashing (20 ms) a stimulus (2° bright spot) in the shared receptive field of both recording locations triggers bursts of spikes in Ipc neurons that are conducted to the paintbrush axonal terminals in the tectum. This activity is recorded throughout a tectal column as prominent tectal OBs (adapted from Marín et al., 2005).

(RtDa) are closely synchronized to the tectal OBs. Furthermore, blocking the paintbrush cholinergic feedback to a given tectal location prevents responses in RtDa to visual targets moving in the corresponding region of visual space. These findings strengthen the hypothesis that cholinergic paintbrushes exert a focalized gating effect, like a "spotlight," on the bidimensional array of dendritic bottlebrushes, enhancing the transmission of incoming visual signals from the optic tectum to higher visual areas.

## Materials and Methods

Experiments were conducted on 42 feral pigeons (300–350 g) of both sexes, obtained from a local dealer and maintained in an institutional facility. All procedures were approved by the Ethics Committee of the Science Faculty of the University of Chile and conformed to the guidelines of the National Institutes of Health on the use of animals in experimental research.

*Surgical procedures.* The pigeons were anesthetized by intramuscular injection of ketamine (75 mg/kg) and xylazine (5 mg/kg), and they were positioned in the standard stereotaxic position (Karten and Hodos, 1967) in a head holder that did not interfere with the animal's visual field. Anesthesia was maintained during surgery and recording by infusing 30% of the initial dose every 2 h via an intramuscular cannula. During the experiment, the electrocardiogram was continuously monitored, and the body temperature of the animal was kept between 38 and 42° by means of a thermoregulated blanket. A small window was opened in the right side of the skull, exposing the dorsolateral part of the tectum and the posterior pole of the telencephalon. To gain access to the central and anterior parts of the isthmi, the telencephalon was gently pushed forward. The dura overlying the tectum and the telencephalic region lying above the rotundus was removed, and the exposed surface was covered with 3% agar saline solution.

*Physiological recordings.* Extracellular recordings were performed in the tectum, the rotundus, and the nuclei isthmi, using tungsten microelectrodes (1–3 MΩ) and two dual-channel amplifiers (model 1800; A-M Systems, Everett, WA). Intracellular recordings were attained in Imc using sharp micropipettes (20–80 MΩ) and a standard intracellular amplifier (NB-100-1; Biomedical Engineering, Thornwood, NY). Micropipettes were pulled from borosilicate glass (0.86 mm inner diameter, 1.5 mm outer diameter; Sutter Instruments, Novato, CA), filled with 2 M potassium acetate. In some cases, 2% biocytin was added to the recording pipette for intracellular filling. Current was injected using 2–5 nA pulses of 0.5 s duration, 50% duty cycle, for 10–30 min, while monitoring the responses of the cell. A chloride silver wire was implanted in the bone in contact with the agar saline as a reference electrode. All structures were approached through the bone window in vertical or oblique penetrations using hydraulic manipulators (David Kopf Instruments, Tujunga, CA).

To investigate whether visually evoked cholinergic feedback in one tectal location is affected by a second focus of visual activity generated in a distant location, bursting activity was recorded extracellularly in two separate sites in Ipc or the tectum, in response to single or sequential visual stimulation (see below). In the case of the Ipc recordings, we used microelectrodes separated by 700–1200 μm in the mediolateral axis. This tip separation and axis orientation corresponded to RFs spaced 40–100° in the ventrodorsal axis of the visual field. For practical reasons, we studied RFs located within a strip of visual space of ~120 by 90°, centered about the optic axis.

To investigate the relationship between the cholinergic feedback to the tectum and visual responses in RtDa, two microelectrodes were positioned in homotopic locations in Ipc and the tectum, whereas a third recording microelectrode was lowered into the dorsoanterior subdivision of Rt.

To transiently inactivate a locus in Imc or Ipc, the recording microelectrodes inserted in each nucleus consisted of a two-barreled glass microelectrode: one barrel containing a sharp tungsten electrode, protruding 15–30 μm; the other barrel, with a tip diameter of 20–30 μm, filled with the AMPA/kainate receptor antagonist CNQX (100 μM in saline). This microelectrode was placed in Imc or Ipc by monitoring the visual responses through the tungsten barrel. Imc or Ipc were then transiently inactivated by injecting 3–10 microdrops (5–20 nl total volume) of CNQX, using a custom-made picospritzer driven by a pulse generator. The inactivation was monitored by recording the neural activity at the injection site. At the end of selected penetrations in the isthmi, marking lesions were made by passing 4 μA of positive current for 4 s through the tungsten barrel. In some experiments, we substituted a rhodamine solution (5% in saline) for the tungsten wire, to mark the injection site as well as to record spike activity.

*Visual stimulation.* Visual stimulation consisted of small (0.5–5°) bright spots presented on a video monitor placed 30–50 cm from the pigeon's eye. After mapping the RFs of the two recording sites in Ipc with a hand-held laser beam, spots were moved within the RFs at 10–50°/s, using a computer-based stimulus generator synchronized to the recording system (Leonardo; Lohmann Research Equipment, Castrop-Rauxel, Germany). RFs were stimulated one at a time, simultaneously, or sequentially. In the last case, a second spot started to move while the first was midway through its movement.

*Data acquisition and analysis.* All physiological data were sampled continuously at 20 kHz using a standard personal computer with a 16-channel analog-to-digital converter board (National Instruments, Aus-

tin, TX); data acquisition and off-line analysis were performed using the Igor Pro 5.0 (WaveMetrics, Lake Oswego, OR) software environment.

Recordings in Ipc using metal electrodes display large-amplitude bursting responses, elicited by stimulating a circumscribed RF (15–25° in diameter), whose position in visual space varies systematically according to the retinotopic map of the nucleus. These bursting responses are mixed with high-frequency (HF) background activity elicited from large parts of the visual field. In a previous study (Marin et al., 2005), we showed that the bursting responses represent the firing of Ipc neurons surrounding the electrode. Evidence presented in this study indicates that the background activity is mostly produced by the firing of Imc axons in Ipc.

Bursting responses attributed to Ipc neurons were separated from background activity and counted using an algorithm written in Igor Pro 5.0, which executed the following procedure: After digital filtering (300 Hz to 10 KHz), spike activity was rectified, smoothed and its envelope defined using a polynomial fit procedure. Then the peaks of the envelope were found and displayed on the screen. Individual bursts, corresponding to peaks greater than a threshold defined for each recording site, were counted and stored. Only bursting activity well isolated from the background was used for this analysis. Raster displays and cumulative histograms were also constructed considering bursts as multiunit events (see Fig. 3). To that end, filtered traces were directly passed through an amplitude-based window discriminator and all peaks greater than a threshold were counted as separate events.

To cross-correlate single-unit activity in Imc with high-frequency activity in Ipc, spike-triggered averages (STAs) were computed using the spikes as trigger sources. To test the validity of the STAs, the data were shuffled by triggering averages using spikes of the subsequent trial.

To cross-correlate the HF activity recorded at two separate sites in Ipc, cross-correlograms were computed between several simultaneously recording segments of 300 ms in which the visually evoked HF activity had constant amplitude.

The coherence of the HF activity in a given segment was defined by dividing the amplitude of the dominant frequency in the Fourier transform of the segment (measured as the integral in the 50 Hz interval centered around the peak frequency) by the total energy in the 300 Hz to 1 kHz range. The coherence was correlated with the root mean square amplitude of the HF activity in the segment.

To evaluate the multiunit activity in Rt, 12 recording traces for each stimulus condition were digitally filtered (300 Hz and 10 kHz), rectified, and smoothed by a running average procedure, which replaced each point value with the average value of neighboring points within a 50 ms window. This procedure is analogous to computing the spike density function, which is normally used to estimate the instantaneous firing pattern in single-unit recordings (Szucs, 1998). The 12 smoothed traces were then averaged, and the result was displayed along with the SE of each averaged point.

*Histological procedures.* In cases in which biocytin had been intracellularly injected, 2–7 h after the injection, the animal was perfused via the carotids under deep anesthesia, using 300–500 ml of avian Ringer's solution, followed by 500 ml of a cold (10°C) solution of 4% paraformaldehyde in 0.1 M phosphate buffer, pH 7.4. The brains were then excised, postfixed overnight, and transferred to 30% sucrose for 3 d, after which the brains were cut in 45–60 $\mu$m coronal sections and processed (ABC Elite kit; Vector Laboratories, Burlingame, CA). In cases in which marking lesions had been made, the animals were given a 1 or 2 d survival period, and, after perfusion, the brains were processed with a standard Nissl or Giemsa protocol. Marking rhodamine injections were located in nondehydrated unstained sections. In all cases, serial sections were examined and photographed using a conventional microscope (BX 60; Olympus Optical, Thornwood, NY), equipped with epifluorescent illumination, and coupled to a Spot digital color camera (Diagnostic Instruments, Sterling Heights, MI).

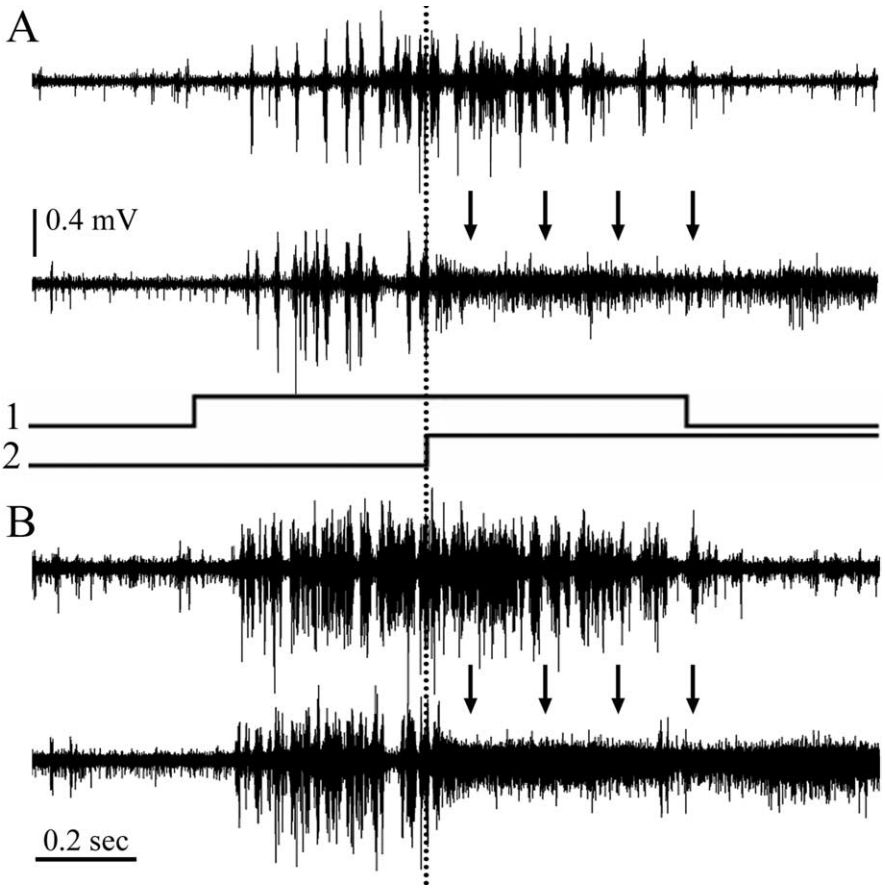


**Figure 2.** Long-distance suppression of bursting activity in Ipc. ***A***, Top trace, Extracellular recording of bursting activity in Ipc evoked by moving a 2° spot at 45°/s for 1 s (signal trace 1), inside the receptive field. Bottom trace, Same recording location as above but with a second spot of the same size and velocity but 100° higher in the visual field, which began to move when the first stimulus was halfway through its course (signal trace 2). This suppressed the bursting responses from the first spot. Suppressed bursting activity is replaced by high-frequency firing of lower amplitude (arrows). ***B***, Superposition of five traces (stimuli as in ***A***) illustrates the robustness of the phenomenon.

## Results

### Wide-field inhibitory interactions in Ipc

We found that the visual responses in Ipc to a moving spot are strongly inhibited if another, distant spot started to move. As shown in Figure 2, moving a bright spot inside the mapped RF (15–25° in diameter) of an Ipc multiunit recording elicited strong bursting discharges, lasting as long as the duration of the stimulus. When a second similar spot, distant from the first, began to move while the first stimulus was in the middle of its trajectory, the bursting response to the first stimulus ceased or diminished significantly ($n$ = 15, 8 pigeons). Remarkably this inhibition could be elicited by moving spots of $<1°$, at visual locations up to $>100°$ away from the first RF.

Recording from two separated loci in Ipc ($n$ = 12, 7 pigeons) showed that, when the respective RFs were stimulated

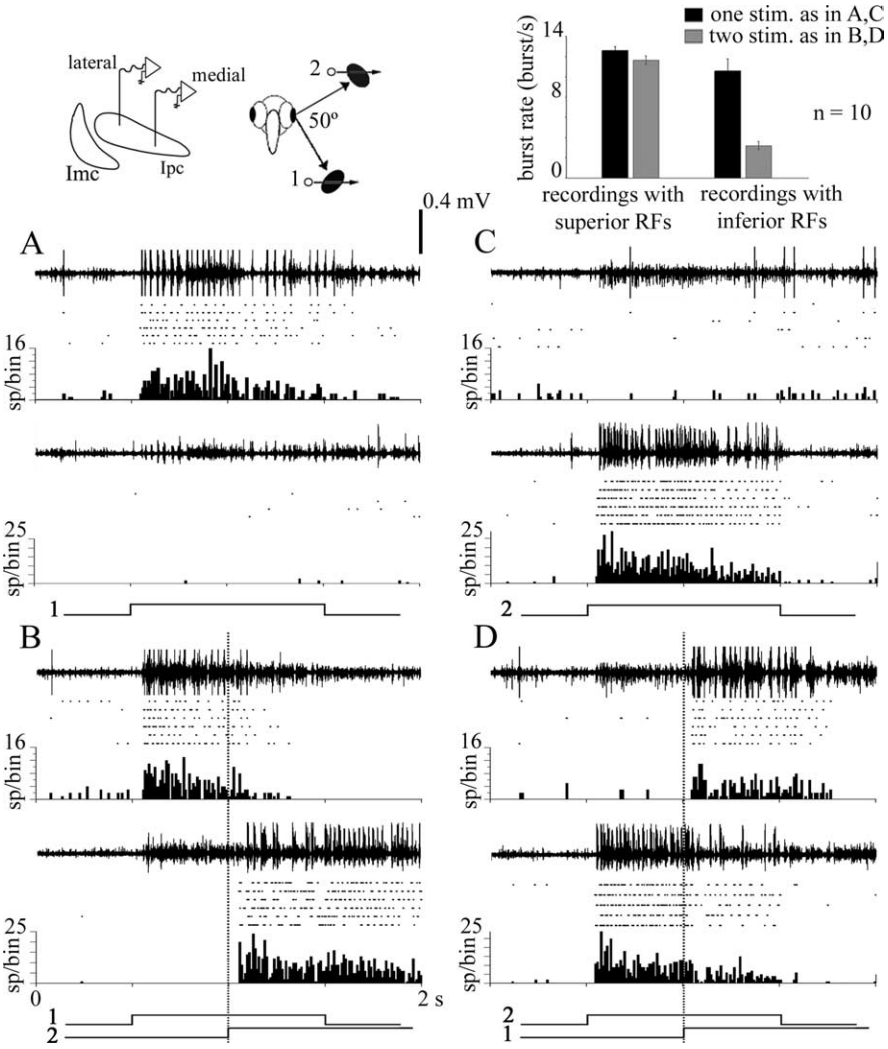


**Figure 3.** Suppressive interactions in Ipc are asymmetric. Dual extracellular recordings of bursting activity in Ipc with tungsten electrodes separated by 0.75 mm in the mediolateral axis. As shown in the schematic, the respective RFs were separated by 50° in the inferior–superior axis. In each panel, the top trace corresponds to the medial recording site (inferior RF), and the bottom trace corresponds to the lateral recording site (superior RF). Below each trace, rasters and cumulative peristimulus time histograms are displayed for six repetitions of each stimulus. Bursting activity elicited from the corresponding RFs was separated from background activity using an amplitude-based window discriminator. The stimulus consisted of either a 2° bright spot moved at 10°/s, for 1 s, within each RF, or of two such spots, the second starting to move when the first was in the middle of its trajectory, as shown by the signal traces underneath each panel. ***A***, Moving a spot in the inferior RF (1) elicited strong bursting responses in the medial recording site. ***B***, Moving a second spot in the superior RF (2) suppressed the responses to the first spot in the medial recording site ( $p < 0.001$, paired *t* test) and elicited strong bursting responses in the lateral recording site. ***C***, Moving a spot in the superior RFs (2) elicited strong bursting responses in the lateral recording site. ***D***, Moving a second spot in the inferior RF (1) produced a much weaker but significant suppression of the response to the first spot in the lateral recording site ( $p < 0{,}001$, paired *t* test). Inset, Summary of results for 10 repetitions of this experiment, in six animals, for RFs separated by 45–100°. Central and superior RFs exerted a strong suppression on bursting responses of inferior RFs, whereas the reverse stimulation produced weak inhibition (both differences were highly significant, $p < 0.005$, paired *t* test).

sequentially, the suppression of bursting responses in the first stimulated location was concurrent with strong bursting responses elicited at the second stimulated location (Fig. 3*A*,*B*). In some cases, the bursting activity completely shifted from one Ipc location to the other. The suppression of bursting responses in one location mostly coincided in time with the start of bursts at the second location, although the latency of the inhibition with respect to the beginning of the second stimulus was variable (35–100 ms).

The inhibition of activity at one location by visual stimulation at the second location was asymmetric. When presented as second stimuli, moving dots in central and superior RFs always inhibited responses in inferior RFs, within the visual strip investigated (Fig. 3*A*,*B*, summarized in bar graph) (67% average inhibition; paired *t* test, $p < 0.005$; $n = 10$). Stimulation of inferior RFs induced much less inhibition on bursting responses from central and superior RFs (Fig. 3*C*,*D*, summarized in bar graph) (8% average inhibition; paired *t* test, $p < 0.005$; $n = 10$) unless the former were near the horizontal meridian, that is, in a less inferior position. In cases in which both RFs were in the central or the superior visual field, the second stimulus usually suppressed the first. When the two stimuli started to move at the same time, both responses were decremented, with a greater or complete suppression of the loci inducing less inhibition in the sequential condition. Identical results were obtained in dual recordings of tectal OBs (18 dual recordings in four pigeons; data not shown), a reflection of the fact that tectal OBs are a manifestation of the bursting firing of Ipc paintbrush terminals in the tectum (Marín et al., 2005).

The suppression of bursting firing of one Ipc locus by a second visual stimulus was usually associated with the appearance of a characteristic form of HF activity recorded at the suppressed loci, which lasted as long as the second stimulus (Fig. 2). This activity consisted of a negative phased (100–400 $\mu$V), spike-like discharge, with a dominant frequency of 500–700 Hz. It only appeared during visual stimulation and was clearly generated by neural elements different from the neurons producing the central bursting responses. This HF activity is also elicited when a single spot moves beyond the borders of the central RF (Marín et al., 2005, their Fig. 5*E*).

Several observations support the hypothesis that HF activity is produced by the synchronized firing of the widespread Imc terminals in Ipc and therefore reflects the inhibition mechanism of the central bursting response by a peripheral stimulus (Marín et al., 2005). First, in a given Ipc locus, the strongest HF activity is elicited by visual stimulation of the central and superior parts of the visual field, the same regions inducing strong suppression of Ipc neurons with RFs in the inferior visual field. Second, the HF activity was in almost perfect phase synchronization between two Ipc recording electrodes separated by >1 mm in Ipc, approximately half the size of the nucleus (Fig. 4) (eight pairs of sites in eight pigeons). Cross-correlograms computed for these dual recordings revealed time shifts of <0.5 ms. More importantly, spikes of Imc neurons were closely synchronized to HF activity recorded in Ipc, and Imc inactivation eliminated HF activity in Ipc (see below).

### Wide-field interactions in Ipc are mediated by Imc

Recordings from Imc neurons confirmed that they were the source of the HF activity recorded in Ipc. Extracellular and intracellular recordings (15 and 4 cases, respectively) showed these neurons to be very sensitive to motion across their highly elongated RFs (15–20° wide and 80–120° high), oriented vertically with respect to the animal's normal head position (Fig. 4*A*,*B*) (Wang and Frost, 1991; Li et al., 2007). Stimulation of RFs in the central and superior parts of the visual field elicited high-frequency (500–700 Hz) spike trains, similar to the HF activity recorded in Ipc. Stimulation of RFs in the inferior visual field provoked lower-frequency spike trains or bursting responses. Simultaneous recordings from Ipc (extracellularly) and from Imc neurons (eight extracellularly and four intracellularly, two labeled with biocytin), showed that high-frequency neuronal firing in Imc is synchronized at the submillisecond level with HF activity in Ipc (Fig. 4*C*,*D*). This was also evident using fine pipettes in "quasi" intracellular recordings from Imc axons within Ipc itself (35 units) (Fig. 4*B*,*D*). Responses from Imc axons were easily identified by their highly elongated, vertically oriented RF, in contrast to the round or oval RFs of Ipc units, and by the stability of the recordings, apparently a consequence of their tolerance to penetration damage. In two cases, injecting biocytin into these units stained axonal fragments in Ipc that had the characteristic Imc wide-field profile.

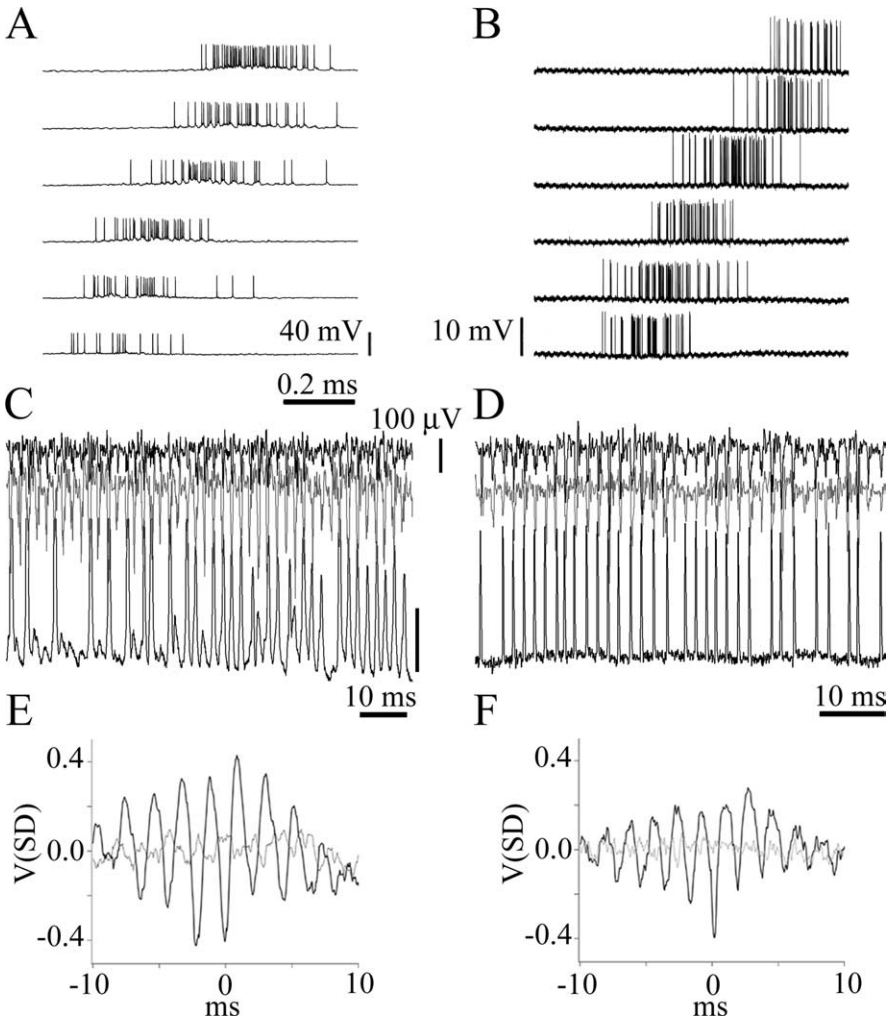


**Figure 4.** High-frequency extracellular activity in Ipc is produced by the synchronized firing of Imc terminals. ***A***, Intracellular recording from a neuron in Imc in response to a 2° bright spot moved at 45°/s in horizontal sweeps in the temporal to nasal direction. Each sweep is 8° lower than the trace above it. In the stereotaxic orientation of the pigeon, the RF of this unit is an elongated diagonal strip of 20° × 80° length, which exceeds the borders of the visual stimulating screen (44°). ***B***, Example of an Imc axon responding with similar characteristics to the same stimulation used in ***A***. ***C***, Simultaneous intracellular recording from a neuron in Imc (bottom black trace; calibration bar, 20 mV) and extracellular recordings from two sites, 0.75 mm apart, in Ipc (top black and gray traces). Note that the high-frequency activity from the two recording sites in Ipc is completely synchronized with each other and with the Imc neuronal spikes. ***D***, Simultaneous recording from an Imc axon (same axon as in ***B***, bottom black trace) and from two sites in Ipc (1 mm tip separation, top black and gray traces) illustrating the same synchronization. ***E***, ***F***, Spike-triggered averages (black lines) of the high-frequency activity traces using the cell and the axon spikes as trigger events. Light gray lines correspond to STAs for shuffled traces.

Two observations indicated that neighboring Imc neurons discharged in synchrony at regular intervals, especially during high-frequency episodes. First, spike interval histograms calculated for well isolated single cells or axons showed two or three secondary peaks regularly spaced by multiples of 1.5–1.8 ms, equivalent to 500–700 Hz. These peaks were also observed in multiunit recordings when two or three discernible individual spikes were pooled (Fig. 5). Second, during high-frequency firing episodes, individual spikes merged into the larger spikes that generated the high-frequency activity (Fig. 5, arrows). In addition, the amplitude and the coherence of the HF activity were closely related: the larger the peak-to-peak amplitude of this activity, the higher its coherence, measured as the relative amplitude of the dominant frequency of its Fourier transform ($r = 0.82$; $p < 0.005$). This close relationship was also seen on visual inspection of the records, because the HF activity was more regular and constant when its amplitude was larger.

To directly test whether Imc neurons mediate long-range suppressive interactions among active locations in Ipc, we inactivated local regions of Imc. Micropipette injection of 5–20 nl of CNQX (100 $\mu$M) reversibly eliminated Imc visual responses recorded with the same electrode used to inject the drug for 3–10 min (10 experiments on 10 pigeons). This Imc local inactivation also eliminated HF activity in Ipc elicited by stimulating a strip of the visual field corresponding to the RFs of the inactivated neurons in Imc. The elimination of HF activity from the inactivated visual strip was observed across recording locations throughout the Ipc nucleus, including simultaneous recordings with separate electrodes (0.75–1 mm tip separation, six cases). When a spot was moved through this visual strip, it still triggered prominent bursting responses at the corresponding Ipc locus, but it induced much less inhibition and, in one case, no inhibition at all, of the activity elicited by a previously moving spot presented elsewhere (Fig. 6). On average, burst suppression diminished from a value of 84% before the drug injection to a value of 50% while the CNQX was acting (Fig. 6, inset) and recovered in parallel with the Imc visual responses in the inactivated site (Fig. 6*G*).

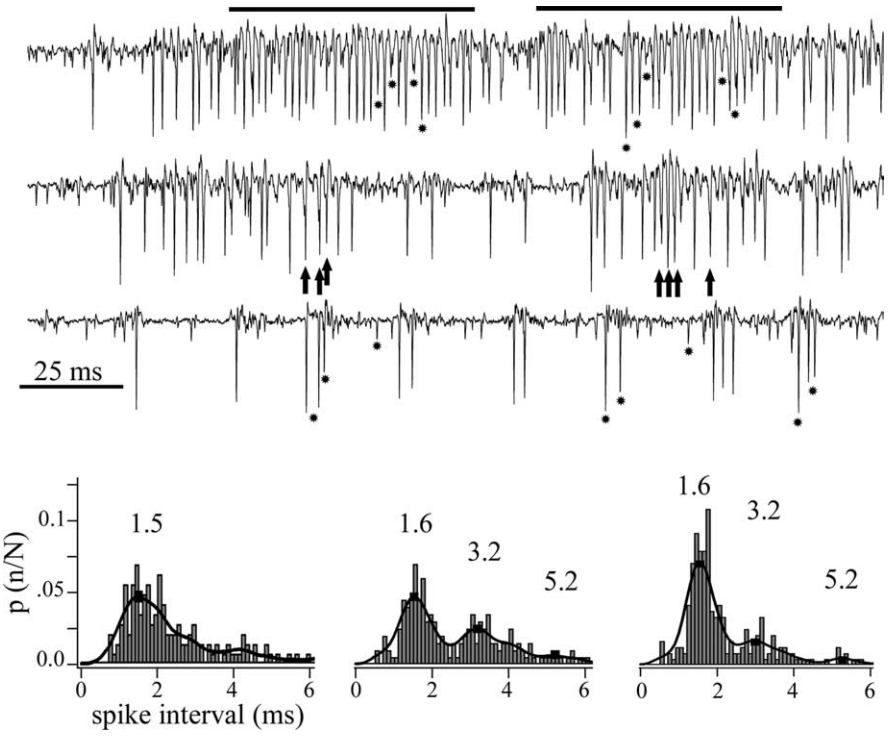


**Figure 5.** Imc neurons fired spikes at regular intervals during high-frequency episodes. Extracellular recordings of spikes from one site in Imc, evoked by the movement of a 2° bright dot along the major axis of the collective RF. The traces show examples at high, medium, and low spike rates. At low discharge rates (bottom trace), large-, medium-, and small-sized spikes are clearly discernable (asterisks). At intermediate discharge rates (middle trace), individual spikes began to fuse with each other, as noted by small peaks (arrows) within larger, fused spikes. At higher rates (top trace), more spikes merged into long-lasting episodes of a regular high-frequency discharge (indicated by the horizontal bars), in which individual and fused spikes tended to appear at regular time intervals. Bottom, Collective interspike interval histograms for each level of average discharge rate shown above. Note that, at intermediate (center) and high (right) discharge rates, secondary peak intervals appear that are near multiples of the most frequent one (1.6 ms, corresponding to 600 Hz). To compute the interspike interval, spikes were sorted from the background using a window discriminator with an algorithm that rejected peaks separated by $<$0.5 ms.

### Local inactivation of Ipc impaired visual transmission to RtDa

To investigate the modulation by Ipc of the ascending flow of visual activity from the optic tectum to RtDa, we blocked visually evoked bursting responses in small regions of Ipc using microinjections of CNQX (5–20 nl, 100 $\mu$M). This procedure eliminated, in a reversible manner, the visually evoked cholinergic feedback to circumscribed regions of the tectum. The effectiveness and time course of this blocking procedure were assessed by recording the tectal OBs with a microelectrode in the homotopic tectal location. By placing a second microelectrode 1–2 mm away from that electrode, we estimated the maximal spatial extent of the blockade. A third microelectrode was used to record from RtDa in vertical penetrations crossing through the telencephalon. All microinjections in Ipc and recording locations in RtDa were confirmed by injections of rhodamine and electrolytic lesions; although in two of eight pigeons, it was uncertain whether the recording location was in RtDa or in the central division of Rt.

All recordings in RtDA displayed characteristic bursting discharges in response to moving targets, consisting of multiunit spike bursts riding on a slow positive wave, with interburst frequency ranging from 35 to 50 Hz (Fig. 7). This bursting activity was especially prominent when moving a laser pointer through the collective RF, usually encompassing approximately half of the visual field.

Across the set of recordings, tectal OBs and RtDa responses were conspicuously synchronized throughout the presentation of the visual stimulus. This synchronization was especially evident when comparing tectal OBs and the positive wave in RtDa, as shown by spike-triggered averages of wide-band RtDa recordings, using the spikes of the tectal OBs as trigger events (Fig. 7). Multiunit spike bursts in RtDa were also synchronized to tectal OBs, but synchronization at the single-unit level could not be assessed because of unreliable spike isolation.

Blocking activity in local regions of the Ipc not only eliminated visually evoked bursting responses from the injected region in Ipc and tectal OBs from the homotopic locus in the tectum but also eliminated responses in RtDa to moving targets in the corresponding part of the visual field (Fig. 8). Spike activity and the slow positive wave were both eliminated by this procedure. In eight cases analyzed quantitatively (in eight pigeons), the average visual spike activity dropped to the baseline when the moving target crossed the RF region corresponding to the blocked region. As assessed by the second recording electrode positioned in TeO, the CNQX doses used in this study eliminated or strongly decremented tectal OBs from a region ranging from 1 to 1.5 mm in diameter, representing 20–30° of the visual field. An equivalent region of the visual field was silenced in RtDa (Fig. 8). In addition, larger injections of CNQX increased the spatial extent and duration of inhibition in RtDA and TeO. Both responses recovered together 5–15 min after drug injection.

Comparable volumes of saline injected in Ipc (two cases) did not produce measurable effects in TeO or in RtDa. Conversely, injections of picrotoxin (5–20 nl, 100 $\mu$M, three cases in two pigeons), a GABA antagonist, increased the amplitude of tectal OBs as well as the bursting profile of RtDa responses evoked by moving targets in the corresponding visual region (data not shown).

## Discussion

In this study, we found that the cholinergic feedback from Ipc to the tectum activated by a moving stimulus has an attention-like property, in that adding a second moving stimulus shifts the focus of this feedback from the first activated location to the second activated location. This is accomplished by inhibitory interactions mostly mediated by the Imc, which sends a wide-field GABAergic projection to Ipc and TeO. Furthermore, two sets of findings reveal that this cholinergic feedback influences the ascending output of the tectum. First, visually evoked extracellular responses recorded in the RtDa, receiving input from TeO, are closely synchronized to this feedback signal, and second, local inactivation of Ipc prevents visual responses in RtDa from occurring in the corresponding region of visual space. These findings further support the hypothesis that active cholinergic paintbrushes exert a focal attentional effect on the tectal visual map, by gating responses in a spatially restricted manner.

**Wide-field inhibitory interactions in Ipc**

Bursting responses in Ipc and OBs in the tectum, evoked by moving a small visual stimulus, was diminished or totally suppressed by an identical second stimulus presented far away in the visual field. A classic linear, suppressive mechanism would require significant spatial summation to produce a comparable effect. The suppression of responses in one location was concurrent with the appearance of responses in the second location, generating a shift in the focus of the cholinergic feedback toward the newly presented stimulus. Surprisingly, these inhibitory interactions were very asymmetric, such that visual stimulation in central and superior RFs inhibited inferior RFs more than the reverse. Although it is possible that this asymmetry may vary under different stimulus conditions, ground feeders, like pigeons, might be predisposed to favor stimuli moving above the horizon.

When bursting responses at a given Ipc recording site were suppressed, they were usually replaced by sustained, high-frequency (500–700 Hz) activity. We provided strong evidence that this activity arises from the synchronized firing of terminals in Ipc of axons from Imc. First, similar high-frequency activity evoked from the same regions of the visual field was recorded extracellularly in Imc. Second, individual Imc spikes tended to fire at interspike intervals defined by the peaks of this activity. Third, simultaneous recordings showed synchronization both between HF activity recorded at widely separated Ipc loci and between this activity and high-frequency firing recorded from Imc neurons and fibers. Finally, inactivation of visual responses in Imc by CNQX eliminated HF activity throughout Ipc from those parts of the visual field represented by the inactivated Imc locations.

The coupling between Imc neurons seems to improve at higher-firing frequencies, because units in Imc merged into multiunit HF activity of larger amplitude, which also become dominated by a narrower range of frequencies. It has been reported that synapses, presumably glutamatergic, between tectal shepherd-crook neurons and their Imc neuronal targets are punctuated with gap junctions (Tömböl and Németh, 1998; Hellmann et al., 2001), which may permit electrical coupling. Interestingly, Imc and Ipc neurons are surrounded by a neuropil enriched with kv3.1 potassium channels (Wang et al., 2006), which in other systems are closely associated with fast postsynaptic currents and high-frequency phase synchronization (Gan and Kaczmarek, 1998; Rudy and McBain, 2001).

Blocking visually evoked responses in Imc with CNQX, in addition to preventing the firing of Imc terminals across Ipc, consistently reduced long-range inhibition between visually activated Ipc locations, indicating that the effect is mediated by the broad terminal fields of Imc axons in Ipc. A similar broad projection from Imc neurons to tectal layers 11 and 12 may duplicate this effect by inhibiting shepherd-crook neurons projecting to Ipc. Interestingly, Imc neurons spread their axonal terminals across TeO and Ipc presumably sparing the regions corresponding to the locus of their visual input (Fig. 1) (Wang et al., 2004), hence facilitating the operation of this network in a winner-take-

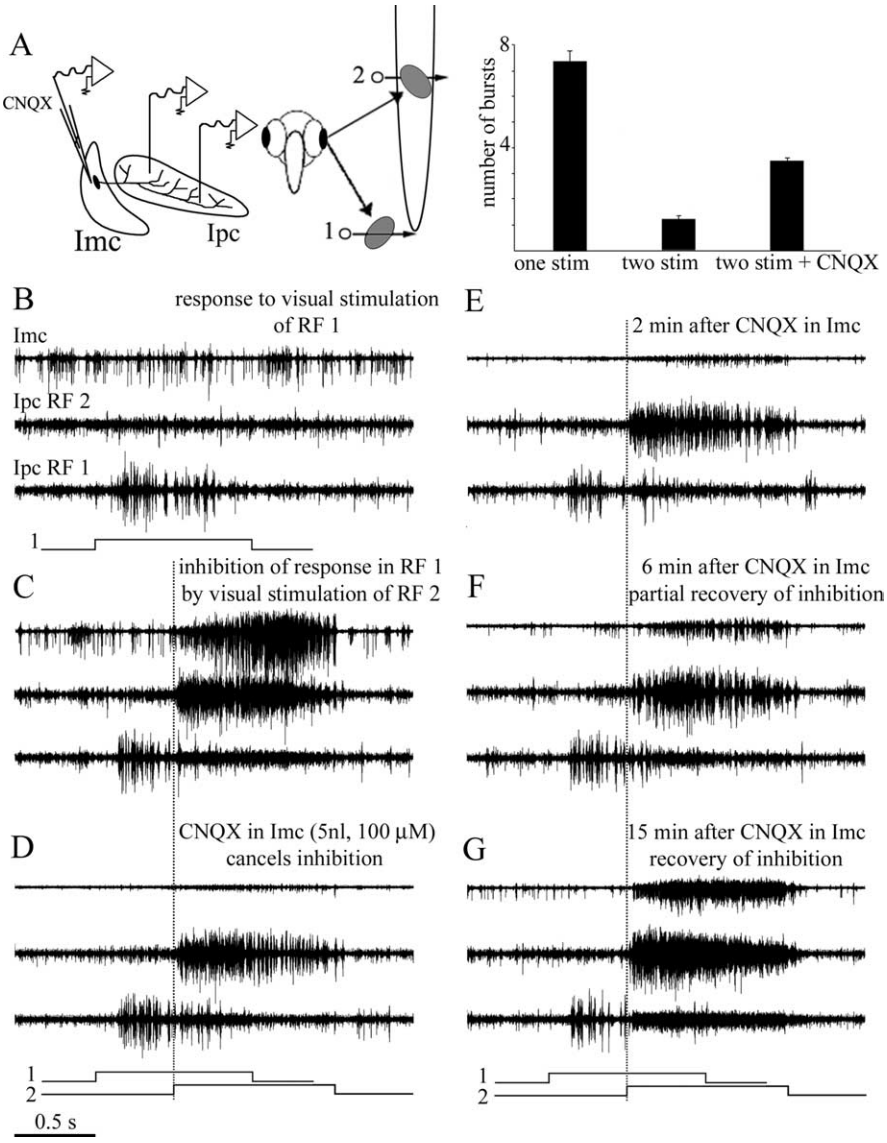


**Figure 6.** Long-distance suppression in Ipc is strongly reduced by Imc inactivation. Two tungsten electrodes were positioned in Ipc in the mediolateral axis, recording multiunit bursting responses from two sites in Ipc. The corresponding RFs were separated by 65° in the inferior–superior axis. A third electrode, for recording and injection, recorded multiunit responses from one site in Imc. ***A***, As shown in the schematic, the collective RF from the Imc site had an elongated RF superimposed to the superior RF (2) of the Ipc. In each panel, the top trace corresponds to the Imc recording, and the middle and bottom traces correspond to the Ipc lateral (RF 2) and medial (RF 1) recording sites, respectively. Each trace represents the superimposed recordings of five stimulus repetitions. The stimulus consisted of one or two 2° bright spot moved at 10°/s within each RF, as shown in the schematic underneath each panel. The dotted vertical line marks the beginning of the movement of the second dot. ***B***, Response to visual stimulus of RF 1 only. ***C***, Movement of a dot in the superior RF (RF 2) strongly suppress the response to the first dot moved in the inferior RF (RF 1). ***D***, Inactivation of Imc by CNQX almost completely cancelled the inhibition shown in ***C***. ***E–G***, The inhibition is reestablished, together with the visually evoked activity in Imc, after ~15 min of recovery. Note that the high-frequency activity in Ipc first diminished with the CNQX application in Imc and then increased during the recovery period. Inset, Summary of results for six repetitions of this experiment in five animals. The cancellation of the induced inhibition provoked by the second stimulus was significantly diminished by the local inactivation of Imc (paired *t* test, $p < 0.005$).

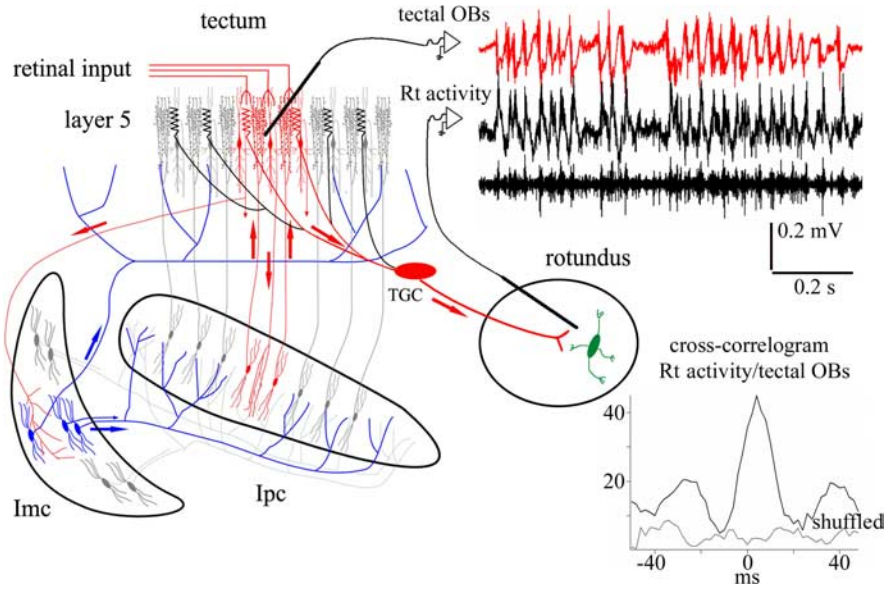


**Figure 7.** Visually evoked activity in RtDa is synchronized with tectal OBs. Recording traces show visually evoked synchronized activity (filtered between 300 and 10 kHz) between the tectal OBs (red trace) and the extracellular activity recorded in the RtDa [filtered between 10 Hz and 10 kHz (top black trace) and between 300 Hz and 10 kHz (bottom black trace)]. Most spikes in Rt ride on a positive slow wave especially prominent when using a laser pointer as a visual stimulus (as in the case illustrated). The inset shows the spike-triggered average of Rt activity (10 Hz to 10 kHz) using tectal bursting spikes as trigger events. The schematic illustrates the isthmi-tectal circuit, including one tectal ganglion cell projecting to RtDa. It suggests that the synchronized activity between tectal OBs and RtDa could be produced by fast paintbrush-mediated cholinergic modulation of the retinal input impinging on the dendritic specializations (bottlebrushes) of TGC tectal neurons.

all manner. Our failure to block the inhibition completely could be explained by insufficient Imc inactivation, because we used small injections to avoid drug diffusion into Ipc, or by the participation of CNQX-insensitive receptors. Conversely, long-range inhibitory interactions may also occur within the tectum, via intratectal GABAergic connections (Luksch and Golz, 2003), and between Imc neurons themselves, as suggested by anatomical (Tömböl and Németh, 1998) and physiological (Wang et al., 2006) evidence.

The winner-take-all mechanism described here for the Ipc feedback may also apply to the third component of the isthmic complex, the nucleus isthmi semilunaris (Slu). Like Ipc, Slu contains cholinergic neurons connecting reciprocally and topographically to TeO and also receives a diffuse GABAergic projection from Imc, presumably from collaterals of axons going to Ipc. Axons from Slu neurons ramify in the tectum in columnar arrangements with denser terminations in the deeper layers and therefore may target a different set of tectal neurons (Wang et al., 2006) (see below).

In mammals, during saccade preparation and shifts of attention, visual activity in target locations of the superior colliculus increases as it decreases in nontarget locations (Glimcher and Sparks, 1992; Kustov and Robinson, 1996; Basso and Wurtz, 1998; McPeek and Keller, 2002), presumably through a winner-take-all process in which the response to a visual stimulus at one location inhibits responses elsewhere (van Opstal and van Gisbergen, 1989). However, Lee and Hall (2006) found no evidence for long-range inhibitory connections in the superior colliculus of mammals, which suggests the possibility that this inhibition occurs elsewhere. The present results indicate that, in the case of the TeO of birds, a winner-take-all mechanism takes place with the participation of the isthmi nuclei, with the Imc mediating long-range inhibition in most of the Ipc and perhaps most of the TeO as well. It is generally agreed that the cholinergic nucleus parabigeminalis (Pbg) of mammals is homologous to the cholinergic isthmi of birds (Diamond et al., 1992). The Pbg has retinotopically organized reciprocal connections with the SC and may modulate neural activity in the superficial layers of the SC in a spatially restricted manner (Graybiel, 1978; Sherk, 1979). Global inhibition could be produced by GABAergic neurons medial to the Pbg that project to the SC (Appell and Behan, 1990; Wang et al., 2004; Lee and Hall, 2006).

### Cholinergic gating of ascending visual transmission

Because Ipc neurons seem to project exclusively to TeO (Wang et al., 2006), the primary effect of Ipc inactivation on visual responses in RtDa should take place in the tectum. A paintbrush-mediated, cholinergic gating of ascending retinotectal transmission could be produced in tectal layer 5, in which Ipc paintbrush terminals intermingle with retinal axon terminals and dendritic bottlebrushes of type I TGCs projecting to RtDa (Wang et al., 2006). One possibility is that the release of ACh in this layer could enhance the release of glutamate from retinal axon terminals by activating presynaptic nicotinic receptors, as has been proposed for teleosts (King and Schmidt, 1991), frogs (Titmus et al., 1999; Dudkin and Gruberg, 2003), and mammals (Binns and Salt, 2000; Salt and Binns, 2000; Lee et al., 2001). A second possibility is that bursting paintbrushes may entrain GABAergic networks, which in turn may facilitate rhythmic bursting responses in their postsynaptic targets, in this case perhaps including dendritic bottlebrushes. Several studies in the mammalian SC and the pigeon tectum indicate that ACh activates GABAergic neurons (Binns and Salt, 2000; Wang et al., 2000; Lee et al., 2001; Endo et al., 2005). Finally, ACh could induce fast excitation directly in the dendritic bottlebrushes. *In vitro* results in the superficial layers of the mammalian SC showed that ACh elicits depolarizing currents in some projecting neurons (Endo et al., 2005). In chick slices, type I TGCs respond with regular sequences of bursts to sustained depolarizations (Luksch et al., 2001). This intrinsic bursting activity could be entrained by the rhythmic modulation of the dendritic inputs to TGCs, resulting from the mechanisms mentioned above. Visually evoked bursting responses from presumptive TCGs have also been recorded *in vivo* (Schmidt and Bischof, 2001). Conversely, we previously reported that some units in tectal layer 13, presumably TGCs, fired with sustained, nonbursting discharges that were not synchronized to tectal OBs (Marín et al., 2005). These responses are more characteristic of type II TGCs (Luksch et al., 2001), which have bottlebrushes distributed in deeper layers and, according to the hypothesis of Wang et al. (2006), might receive an input from the cholinergic terminals arising from Slu.

Ipc inactivation might also influence Rt visual responses by more indirect routes. Rhythmic activity of TGCs entrained by paintbrush activity could synchronize discharges in the GABAergic nuclei of the tectothalamic tract, which receive collateral innervation of the TGCs and project to specific subdivisions in Rt

(Mpodozis et al., 1996). Conversely, paintbrush activity might modulate shepherd-crook neurons projecting to Slu, which seems to send a sparse projection to Rt (Hellmann et al., 2001).

The present results suggest that active paintbrush terminals may act as a spatial pointer that connect global activity in RtDa to specific locations within the fine-grained map of dendritic bottlebrushes of type I TGCs. If a wave front of retinal input arrives to the tectum, a volley of cholinergic feedback will invade the activated location, enabling the ascending transmission of that activity to RtDa. Most neurons throughout RtDa will thus respond to this location with bursting discharges synchronized to the corresponding tectal OBs. If a new stimulus appears in the visual field, this wave front will be diminished or abolished, and a new cholinergic wave front will start at the newly activated tectal location. Bursting responses in RtDa will then be synchronized with OBs from this new location. If paintbrushes are activated in more than one area at once, signal transmission would still be enhanced at locations receiving the strongest feedback, and competition could be resolved in Rt or higher visual areas. Alternatively, each active tectal location might synchronize to separate populations in RtDa, "tagging" in this way several salient items at once (Niebur et al., 1993; Fries, 2005).

The isthmotectal circuitry is similarly organized across vertebrate classes, and several evidence exist for it playing a role in target selection and spatial attention (Sereno and Ulinski, 1987; Gruberg et al., 1991; Winkowski and Gruberg, 2002; Cui and Malpeli, 2003; Wang et al., 2004, 2006; Gruberg et al., 2006; Maczko et al., 2006). TGCs with remarkably similar morphology and central projections also exist in the TeO of most vertebrates. In mammals, TGCs from the inferior part of the superficial layers of the SC form the main ascending pathway to the pulvinar (Major et al., 2000). The present data from the pigeon indicate that a winner-take-all mechanism, mediated by the isthmi, may closely control the ascending flow of retinal signals carried by the TGCs to higher visual areas.

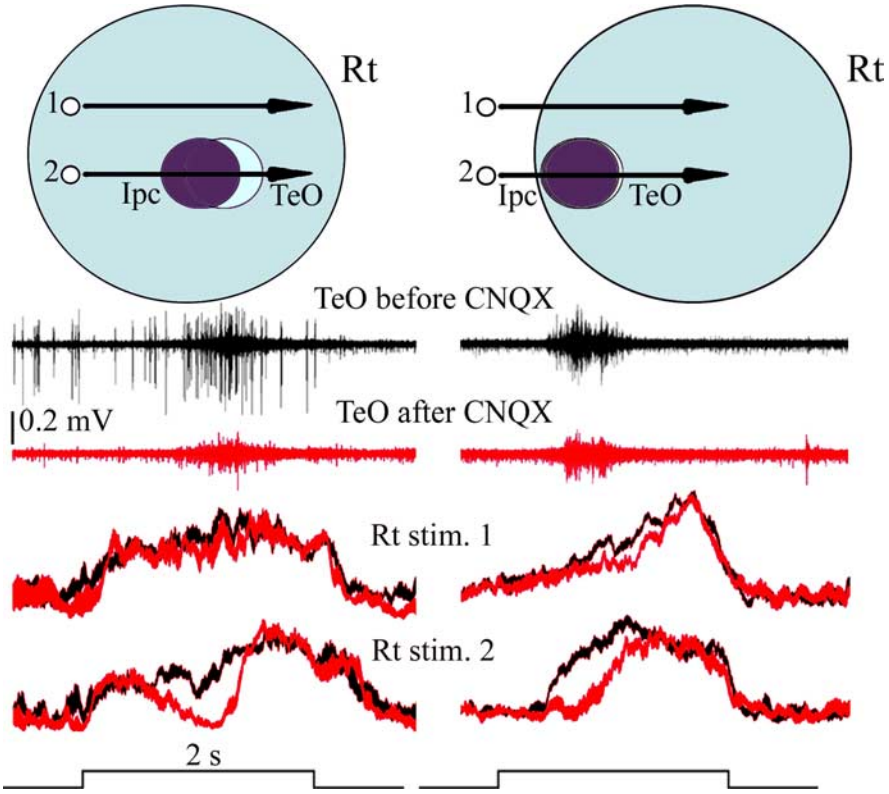


**Figure 8.** Local blockade of the cholinergic feedback to the tectum eliminates visual responses in RtDa from the corresponding location of visual space. Left and right panels illustrate two similar experiments performed in different pigeons. One recording tungsten microelectrode and one dual microelectrode for recording and microinjection were inserted in homotopic locations in TeO and Ipc, respectively, whereas a third microelectrode was inserted in RtDa. Top schematics represent the relative position of the corresponding receptive fields in each case. The stimulus consisted of a bright spot (2°, 44°/s), moved either across the center of the superimposed Ipc and tectal OBs RFs (2) or 20° above (1). Middle traces show tectal OBs in response to stimulus 2 before (dark trace) and after (red trace) injecting CNQX (6–20 nl) in Ipc. CNQX injection eliminates OBs at the tectal recording site. Bottom traces represent visually evoked responses in RtDa, before (dark traces) and after (red traces) CNQX injections in Ipc, to stimuli 1 and 2. Each trace represents 12 individual multiunit recordings, filtered between 300 Hz and 10 kHz, rectified, and smoothed before averaging; trace thickness corresponds to the SE error. Note that Rt activity drops to the baseline after CNQX injection in Ipc when the spot crosses the part of the visual field corresponding to the blocked region (stimulus 2). No effect (left) or a minor effect (right) is observed when the spot is moved above the inactivated field (stimulus 1).

## References


Appell PP, Behan M (1990) Sources of subcortical GABAergic projections to the superior colliculus in the cat. J Comp Neurol 302:143–158.

Basso MA, Wurtz RH (1998) Modulation of neuronal activity in superior colliculus by changes in target probability. J Neurosci 18:7519–7534.

Binns KE, Salt TE (2000) The functional influence of nicotinic cholinergic receptors on the visual responses of neurones in the superficial superior colliculus. Vis Neurosci 17:283–289.

Carello CD, Krauzlis RJ (2004) Manipulating intent: evidence for a causal role of the superior colliculus in target selection. Neuron 43:575–583.

Cavanaugh J, Wurtz RH (2004) Subcortical modulation of attention counters change blindness. J Neurosci 24:11236–11243.

Cui H, Malpeli JG (2003) Activity in the parabigeminal nucleus during eye movements directed at moving and stationary targets. J Neurophysiol 89:3128–3142.

Deco G, Pollatos O, Zihl J (2002) The time course of selective visual attention: theory and experiments. Vision Res 42:2925–2945.

Desimone R, Duncan J (1995) Neural mechanisms of selective visual attention. Annu Rev Neurosci 18:193–222.

Diamond IT, Fitzpatrick D, Conley M (1992) A projection from the parabigeminal nucleus to the pulvinar nucleus in Galago. J Comp Neurol 316:375–382.

Dudkin EA, Gruberg ER (2003) Nucleus isthmi enhances calcium influx into optic nerve fiber terminals in *Rana pipiens*. Brain Res 969:44–52.

Endo T, Yanagawa Y, Obata K, Isa T (2005) Nicotinic acetylcholine receptor subtypes involved in facilitation of GABAergic inhibition in mouse superficial superior colliculus. J Neurophysiol 94:3893–3902.

Fries P (2005) A mechanism for cognitive dynamics:neuronal communication through neuronal coherence. Trends Cogn Sci 9:474–480.

Gan L, Kaczmarek LK (1998) When, where, and how much? Expression of the Kv3.1 potassium channel in high-frequency firing neurons. J Neurobiol 37:69–79.

Glimcher PW, Sparks DL (1992) Movement selection in advance of action in the superior colliculus. Nature 355:542–545.

Graybiel AM (1978) A satellite system of the superior colliculus: the parabigeminal nucleus and its projections to the superficial collicular layers. Brain Res 145:365–374.

Gruberg E, Dudkin E, Wang Y, Marin G, Salas C, Sentis E, Letelier J, Mpodozis J, Malpeli J, Cui H, Ma R, Northmore D, Udin S (2006) Influencing and interpreting visual input: the role of a visual feedback system. J Neurosci 26:10368–10371.

Gruberg ER, Wallace MT, Caine HS, Mote MI (1991) Behavioral and physiological consequences of unilateral ablation of the nucleus isthmi in the leopard frog. Brain Behav Evol 37:92–103.

Hellmann B, Manns M, Güntürkun O (2001) Nucleus isthmi, pars semilunaris as a key component of the tectofugal visual system in pigeons. J Comp Neurol 436:153–166.

Karten H, Hodos W (1967) A stereotaxic atlas of the brain of the pigeon *Columba livia*. Baltimore: Johns Hopkins UP.

Karten HJ, Cox K, Mpodozis J (1997) Two distinct populations of tectal neurons have unique connections within the retinotectorotundal pathway of the pigeon (*Columba livia*). J Comp Neurol 387:449–465.

King WM, Schmidt JT (1991) The long latency component of retinotectal transmission: enhancement by stimulation of nucleus isthmi or tectobulbar tract and block by nicotinic cholinergic antagonists. Neuroscience 40:701–712.

Kustov AA, Robinson DL (1996) Shared neural control of attentional shifts and eye movements. Nature 384:74–77.

Lee P, Hall WC (2006) An *in vitro* study of horizontal connections in the intermediate layer of the superior colliculus. J Neurosci 26:4763–4768.

Lee PH, Schmidt M, Hall WC (2001) Excitatory and inhibitory circuitry in the superficial gray layer of the superior colliculus. J Neurosci 21:8145–8153.

Li DP, Xiao Q, Wang SR (2007) Feedforward construction of the receptive field and orientation selectivity of visual neurons in the pigeon. Cereb Cortex 17:885–893.

Luksch H, Golz S (2003) Anatomy and physiology of horizontal cells in layer 5b of the chicken optic tectum. J Chem Neuroanat 25:185–194.

Luksch H, Cox K, Karten HJ (1998) Bottlebrush dendritic endings and large dendritic fields: motion-detecting neurons in the tectofugal pathway. J Comp Neurol 396:399–414.

Luksch H, Karten HJ, Kleinfeld D, Wessel R (2001) Chattering and differential signal processing in identified motion-sensitive neurons of parallel visual pathways in the chick tectum. J Neurosci 21:6440–6446.

Maczko KA, Knudsen PF, Knudsen EI (2006) Auditory and visual space maps in the cholinergic nucleus isthmi pars parvocellularis of the barn owl. J Neurosci 26:12799–12806.

Major DE, Luksch H, Karten HJ (2000) Bottlebrush dendritic endings and large dendritic fields: motion-detecting neurons in the mammalian tectum. J Comp Neurol 423:243–260.

Marín G, Letelier JC, Henny P, Sentis E, Farfan G, Fredes F, Pohl N, Karten H, Mpodozis J (2003) Spatial organization of the pigeon tectorotundal pathway: an interdigitating topographic arrangement. J Comp Neurol 458:361–380.

Marín G, Mpodozis J, Sentis E, Ossandon T, Letelier JC (2005) Oscillatory bursts in the optic tectum of birds represent re-entrant signals from the nucleus isthmi pars parvocellularis. J Neurosci 25:7081–7089.

Maunsell JH, Cook EP (2002) The role of attention in visual processing. Philos Trans R Soc Lond B Biol Sci 357:1063–1072.

McPeek RM, Keller EL (2002) Saccade target selection in the superior colliculus during a visual search task. J Neurophysiol 88:2019–2034.

Mpodozis J, Cox K, Shimizu T, Bischof HJ, Woodson W, Karten HJ (1996) GABAergic inputs to the nucleus rotundus (pulvinar inferior) of the pigeon (*Columba livia*). J Comp Neurol 374:204–222.

Muller JR, Philiastides MG, Newsome WT (2005) Microstimulation of the superior colliculus focuses attention without moving the eyes. Proc Natl Acad Sci USA 102:524–529.

Niebur E, Koch C, Rosin C (1993) An oscillation-based model for the neuronal basis of attention. Vision Res 33:2789–2802.

Posner MI (1980) Orienting of attention. Q J Exp Psychol 32:3–25.

Rudy B, McBain CJ (2001) Kv3 channels: voltage-gated $K^+$ channels designed for high-frequency repetitive firing. Trends Neurosci 24:517–526.

Salt TE, Binns KE (2000) Contributions of mGlu1 and mGlu5 receptors to interactions with *N*-methyl-D-aspartate receptor-mediated responses and nociceptive sensory responses of rat thalamic neurons. Neuroscience 100:375–380.

Schmidt A, Bischof HJ (2001) Neurons with complex receptive fields in the stratum griseum centrale of the zebra finch (*Taeniopygia guffata* castanotis Gould) optic tectum. J Comp Physiol A Neuroethol Sens Neural Behav Physiol 187:913–924.

Sereno MI, Ulinski PS (1987) Caudal topographic nucleus isthmi and the rostral nontopographic nucleus isthmi in the turtle, *Pseudemys scripta*. J Comp Neurol 261:319–346.

Sherk H (1979) Connections and visual-field mapping in cat's tectoparabigeminal circuit. J Neurophysiol 42:1656–1668.

Szucs A (1998) Applications of the spike density function in analysis of neuronal firing patterns. J Neurosci Methods 81:159–167.

Titmus MJ, Tsai HJ, Lima R, Udin SB (1999) Effects of choline and other nicotinic agonists on the tectum of juvenile and adult *Xenopus* frogs: a patch-clamp study. Neuroscience 91:753–769.

Tömböl T, Németh A (1998) GABA-immunohistological observations, at the electron-microscopical level, of the neurons of isthmic nuclei in chicken, *Gallus domesticus*. Cell Tissue Res 291:255–266.

van Opstal AJ, van Gisbergen JA (1989) Scatter in the metrics of saccades and properties of the collicular motor map. Vision Res 29:1183–1196.

Wang Y, Xiao J, Wang SR (2000) Excitatory and inhibitory receptive fields of tectal cells are differentially modified by magnocellular and parvocellular divisions of the pigeon nucleus isthmi. J Comp Physiol A Neuroethol Sens Neural Behav Physiol 186:505–511.

Wang Y, Major DE, Karten HJ (2004) Morphology and connections of nucleus isthmi pars magnocellularis in chicks (*Gallus gallus*). J Comp Neurol 469:275–297.

Wang Y, Luksch H, Brecha NC, Karten HJ (2006) Columnar projections from the cholinergic nucleus isthmi to the optic tectum in chicks (*Gallus gallus*): a possible substrate for synchronizing tectal channels. J Comp Neurol 494:7–35.

Wang YC, Frost BJ (1991) Visual response characteristics of neurons in the nucleus isthmi magnocellularis and nucleus isthmi parvocellularis of pigeons. Exp Brain Res 87:624–633.

Wang YC, Jiang S, Frost BJ (1993) Visual processing in pigeon nucleus rotundus: luminance, color, motion, and looming subdivisions. Vis Neurosci 10:21–30.

Winkowski DE, Gruberg ER (2002) The representation of the ipsilateral eye in nucleus isthmi of the leopard frog, *Rana pipiens*. Vis Neurosci 19:669–679.